Available online at www.sciencedirect.com
SCIENCE DIRECT®
PERGAMON
Polyhedron 22 (2003) 2647–2653
POLYHEDRON
www.elsevier.com/locate/poly

Synthesis and characterization of Keggin P–Mo–V heteropolyanion and its Langmuir–Blodgett film

Li-Feng Zhong, Yuan-Ming Zhang *, Yu Tang, Yan Bai

Department of Chemistry, Ji'Nan University, Guangzhou 510632, China

Received 17 March 2003; accepted 12 May 2003

Abstract

The divanadium-substituted molybdophosphate acid, $H_5PMo_{10}V_2O_{40}\cdot 13H_2O$ was synthesized by acidification-etherate. It was proved that the obtained compound has the Keggin structure. A Langmuir–Blodgett (LB) film with the $PMo_{10}V_2O_{40}^{5-}$ heteropolyanion in the subphase was formed. Remarkable modifications of the compression isotherms indicate that the heteropolyanion interacts with the octadecylamine hydrochloride (ODA) monolayer. Atomic force microscopy (AFM), low-angle X-ray diffraction (LAXD), FT-IR and UV spectroscopy were used to investigate the morphology and molecular structure of the deposited ODA/$PMo_{10}V_2O_{40}^{5-}$ LB film. The cyclic voltammetric (CV) behavior of the $PMo_{10}V_2O_{40}^{5-}$ heteropolyanion and the LB films of ODA/$PMo_{10}V_2O_{40}^{5-}$ deposited onto a glassy carbon electrode were studied.

Keywords: Heteropolyanion; Keggin structures; LB films; Cyclic voltammetry

1. Introduction

The study of heteropoly compounds has attracted much attention in material science, catalysis, medicine, and biochemistry recently [1–6]. Especially in the field of electrocatalysis, owing to the ability of heteropolyanions to accept various numbers of electrons to generate mixed-valency species, significant research efforts have been directed to the electrochemical behavior of heteropoly compounds aiming to prepare a new type of catalyst for various applications in heterogeneous and homogeneous electrocatalysis [6–9]. Anson [7] had successfully immobilized metal-substituted heteropolyanions in polypyrrole and studied its electrochemical behavior, but the modified electrode seemed to be degraded easily and the anion was lost. Bidan [10] reported that the modified electrode obtained from poly(*N*-methylpyrrole) shows important electrochemical stability and catalytic activity for the reduction of nitrite. However, these coating techniques often lead to a random orientation of redox sites in the film. As a reasonable attachment method for improving the ordering and properties of such a multilayer film, the Langmuir–Blodgett (LB) technique may be a useful choice [11–13].

In the present study, a transition-metal-substituted heteropoly acid was synthesized and characterized through various physical methods. LB films containing such a heteropolyanion have been characterized by cyclic voltammetric (CV), atomic force microscopy (AFM), low-angle X-ray diffraction (LAXD), FT-IR and UV. These results indicate that using this method, an ultrathin film with regularity in molecular organization can be obtained. This new type of film can be exploited for extensive applications in electrocatalysis and as sensors and photoelectron-chemical devices.

2. Experimental

2.1. Chemicals

Octadecylamine hydrochloride (ODA) and $NaVO_3$ were commercially obtained from Alfa Aesar. Chloroform was used as a spreading solvent and was redistilled

* Corresponding author. Tel.: +86-20-8522-6273; fax: +86-20-8522-6262.
E-mail address: tzhangym@vip.163.com (Y.-M. Zhang).

0277-5387/03/$ - see front matter © 2003 Elsevier Ltd. All rights reserved.
doi:10.1016/S0277-5387(03)00370-X

before use. All other chemicals were of analytical grade and used as received. Water was distilled twice before use.

2.2. Instruments

The elemental analysis of P, Mo, V was carried out by IRIS Advantage (HR) inductively coupled plasma atomic emission spectroscopy (ICP-AES) (TJA Co., USA). Thermal decomposition behavior was studied by a TG 209 thermal analyzer (Netzsch Co., Germany) and N_2 was used as the atmosphere. XRD and LAXD experiments were performed with a D/max-3A model X-ray powder diffractometer (Rigaku Corporation, Japan). FT-IR spectra were recorded in a Bruker EQUINOX 55 spectrometer using KBr pellets. UV spectra were obtained with an UV-2501 PC UV-Vis Recording Spectrophotometer (Shimadzu Corporation, Japan). AFM images were obtained with an Autoprobe CP Research model from THERMO MICROSCOPE (USA) instruments with a APSC-0100 model scanner. The tapping imaging model was used. Measurement of surface pressure–area (π–A) isotherms and preparation of LB films were carried out with a WM-2 Langmuir trough system, which is a fully computerized and programmable apparatus fitted with two movable Teflon barriers. Electrochemical measurements were conducted on a BAS-100B electrochemical system (BAS Co., USA). A three-electrode, one-compartment cell was used with a glassy carbon working electrode, platinum wire counter-electrode and an Ag/AgCl/sat. KCl reference electrode.

2.3. Preparation of the compound

Divanadium-substituted Keggin-type molybdophosphate acid, $H_5PMo_{10}V_2O_{40}\cdot 13H_2O$ (abbreviated to $PMo_{10}V_2$) was synthesized according to Ref. [14].

2.4. Preparation of $ODA/PMo_{10}V_2O_{40}^{5-}$ LB films

The measurements of the surface pressure-area isotherm and the deposition of the LB film were carried out at 25 ± 1 °C. The monolayer of the ODA was formed by spreading out a 1.0×10^{-3} mol l^{-1} ODA chloroform solution onto a 1.0×10^{-5} mol l^{-1} $PMo_{10}V_2$ aqueous solution (subphase) with pH 5.1. The compression was performed using a constant speed for the barrier of 10 mm min^{-1}. Assembled Y-type film has been obtained by the vertical lifting mode method using the lifting speed of 2 mm min^{-1}. The monolayer was transferred onto quartz substrates and a glassy carbon electrode which was treated with dichlorodimethylsilane at a constant surface pressure of 20 mN m^{-1}. All the LB films are each composed of 12 layers. The obtained LB films were placed vertically in a beaker and isolated from air by a seal film. The following series of characterizations indicate that the transfer ratio is up to about 0.95 on lifting film using a surface pressure of 20 mN m^{-1}, and the multilayer is very stable.

3. Results and discussion

3.1. TG analysis and ICP-AES

The main element contents were analyzed by ICP-AES. Found (calculated): P, 1.51 (1.57); Mo, 47.72 (48.68); V, 4.89 (5.17). The atom ratio of P:Mo:V is equal to 1:10:2. The water content was determined by thermogravimetry. The TG curve of the product show that there are three different steps of mass loss. Between 25 and 62.4 °C 4.48 wt.% crystallized water is lost. 7.29 wt.% associative water is lost in the range 62.4–190.7 °C. The third mass loss of 2.26 wt.% is recorded from 190.7 to 423.8 °C, which represents the loss of structural water. Associated with the loss ratio of the first and second steps and the data of ICP-AES, the number of water molecules was worked out to be 12.8806. The structural formula is thus $H_5PMo_{10}V_2O_{40}\cdot 13H_2O$.

3.2. Monolayers of ODA at the air/water interface

The surface pressure–area isotherms (π–A curves) for ODA on pure water (curve A) and on a 1.0×10^{-5} mol l^{-1} $PMo_{10}V_2$ aqueous solution (curve B) are presented in Fig. 1. ODA can form a stable monolayer not only at the air/water interface but also at the air-aqueous solution of the heteropolyanion interface. In Fig. 1, curve A and curve B have air-phase, liquid-phase and solid-phase segments. The collapse pressure of the monolayer of curve A and curve B are about 33 mN m^{-1} and 32 mN m^{-1} respectively. Drawing the tangent of the solid-phase curve, the area per molecule is 0.31 nm^2 for curve B and 0.19 nm^2 for curve A. When a $PMo_{10}V_2O_{40}^{5-}$ anion is added to the pure water

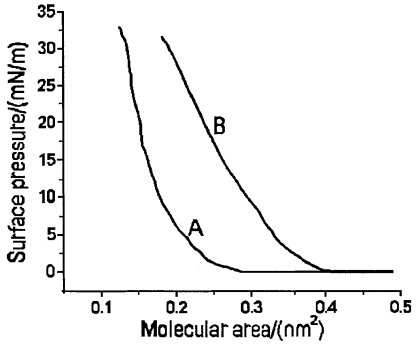

Fig. 1. Compression isotherm of ODA on pure water (A) and on a 10^{-5} M $PMo_{10}V_2$ solution (B).

subphase, the compression isotherm of ODA is progressively modified, as shown by curve B in Fig. 1. The isotherm is shifted to a larger area per molecule and at the same time, the isotherm shows a slower rise. The cross-section area per ODA molecule is about 0.19 nm^2, but the radium of the $PMo_{10}V_2O_{40}^{5-}$ heteropolyanion is 0.5 nm. When a $PMo_{10}V_2O_{40}^{5-}$ anion is added to the subphase, the monolayer of ODA will attach a layer of heteropolyanion by electrostatic interaction, which results in an enlarged cross-section area. On the other hand, because the $PMo_{10}V_2O_{40}^{5-}$ heteropolyanion possesses five negative charges, accompanied by the increase of surface pressure, the strong ionic repulsive interaction brings on a slower rise of the isotherm.

3.3. IR spectra

In the FT-IR spectrum of $PMo_{10}V_2$, there are four characteristic adsorption bands: 1061 cm^{-1} represents the symmetrical stretch vibration of the P–O(a) bond, 962 cm^{-1} indicates the asymmetrical stretch vibration of M–O(d), and the asymmetrical stretch vibration of M–O(b)–M and M–O(c)–M appear at 780 and 865 cm^{-1}, respectively. The four characteristic bands demonstrate that the obtained compound has the Keggin structure [15]. Besides these, there are stretching and bending vibrations of crystallized water at 3420 and 1625 cm^{-1}, respectively. There is no adsorption band from 1100 to 1200 cm^{-1}, which indicates that the heteropoly acid has the Keggin structure, but not the Silverton structure.

The ODA/$PMo_{10}V_2O_{40}^{5-}$ LB film was characterized by FT-IR spectroscopy too. Compared with that of $PMo_{10}V_2$, there is no characteristic band in the range of 1100–700 cm^{-1}, but two medium adsorption bands at 2916.91 and 2849.06 cm^{-1} were observed. Judged from these, there are asymmetric and symmetric stretching vibrations of C–H in long chain alkyl groups. These indicate that an ODA monolayer was deposited on the quartz slide successfully. However, because the quartz slide can almost fully adsorb the radiation below 2065 cm^{-1}, the four characteristic adsorption bands of heteropolyanion from 1100–700 cm^{-1} were covered completely. So the characteristic adsorption bands of the heteropolyanion cannot be observed.

3.4. UV spectra

The UV spectra of 12-layer ODA/$PMo_{10}V_2O_{40}^{5-}$ LB film (curve 2) and the parent solution (curve 1) are presented in Fig. 2. Comparing curve 1 with curve 2, the absorption strength of the parent solution is larger than that of the ODA/$PMo_{10}V_2O_{40}^{5-}$ LB film. Both have two absorption peaks; they are 210.80, 303.20 nm for curve 1 and 230.20, 311.00 nm for curve 2. The former correspond to the charge-transfer transition of $O_d \rightarrow M$ and the later to $O_{b(c)} \rightarrow M$. All the absorption peaks of ODA/$PMo_{10}V_2O_{40}^{5-}$ LB film are red-shifted compared with those of the parent solution. The former shifts by 19.4 nm and the later by 7.8 nm. These indicate that the $PMo_{10}V_2O_{40}^{5-}$ ions are densely packed and oriented orderly in the film. The main reason is that there is electrostatic interaction between the heteropolyanion and the hydrophobic group, which reduces the energy of the charge-transfer transition.

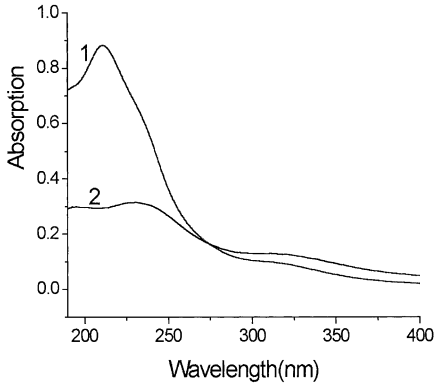

Fig. 2. UV spectra pattern of ODA/$PMo_{10}V_2$ LB film (2) and parent solution (1).

3.5. X-ray diffraction

The result of X-ray powder diffraction of $PMo_{10}V_2$ displays that the diffraction peaks are primarily distributed in four ranges of 2θ which are 7–10°, 16–23°, 25–30° and 33–38°. The intensity of the diffraction peaks of the first range is the highest. In each of the four ranges of 2θ, there is a characteristic peak of the heteropolyanion that have the Keggin structure [16].

The XRD pattern of the ODA/$PMo_{10}V_2O_{40}^{5-}$ LB film deposited on the quartz slide is presented in Fig. 3. The LB film is composed of 12 layers. There are five peaks and the corresponding values of 2θ are 1.30°, 1.72°, 2.16°, 2.74°, and 5.48°. The strongest diffraction peak is at $2\theta = 2.74°$. These demonstrate that the LB film has a lamellar structure and well-defined layers [17].

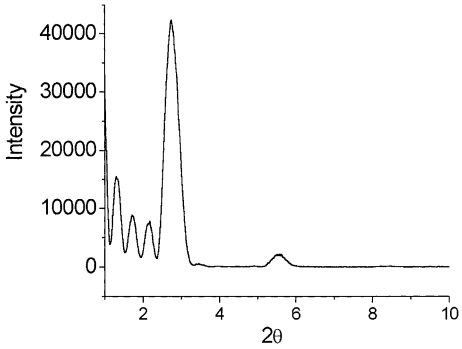

Fig. 3. LAXD pattern of ODA/$PMo_{10}V_2$ LB film.

According to the Bragg equation, the value of d is equal to 6.79 nm. For Y-type film, $d/2$ is just the thickness of a monolayer. It has been known that the length of ODA is 2.4 nm and the radius of this heteropolyanion is about 0.5 nm. So the following conclusions can be drawn: (1) There is one layer of heteropolyanions in the middle of the ODA lamellar structure in the LB film. (2) These heteropolyanions are separated by ODA molecules. (3) The chain of the ODA molecule is almost vertical to the plane of the quartz slide (Fig. 4).

3.6. Morphological observation of ODA/$PMo_{10}V_2O_{40}^{5-}$ LB film

Parts A, B in Fig. 5 display the typical planar and three-dimensional AFM images of the ODA/$PMo_{10}V_2O_{40}^{5-}$ LB film deposited on quartz substrates. Part C in Fig. 5 shows the cross-section of parts A, B in Fig. 5. The particles of heteropoly acid distributed on the ODA monolayer homogeneously was observed from Parts A, B in Fig. 5. The dimension of the particles is 50 nm and the height distributes primarily on 7–8 nm. The homogeneity of the film suggests that the molecules deposited on the substrate are of relatively dense packing, which is similar to the transfer of conventional amphiphilic materials such as fatty acids. It is very important to build ODA/$PMo_{10}V_2O_{40}^{5-}$ LB film supermolecular assemblies with well-defined molecular arrangement and orientation. The average roughness (R_a), the RMS roughness (R_q), the peak height (R_p) and the valley height (R_v) are equal to 4.247, 1.754, 3.531, and −3.094 nm, respectively from Part C. On the other hand, the average roughness of 4.247 nm also demonstrates that even for a 12-layer LB film of ODA/$PMo_{10}V_2$, an extremely regular surface morphology was observed over the large scale (1 × 1 μm) and did not display any evidence for the existence of domain structures.

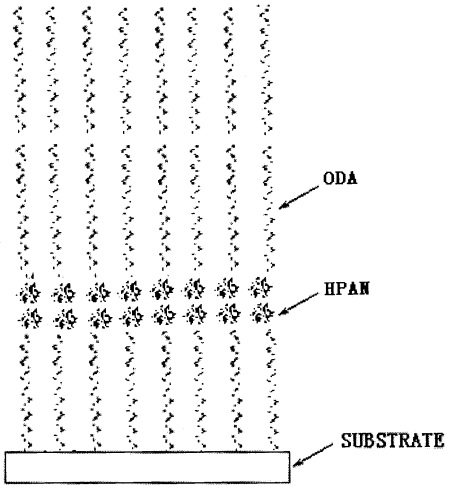

Fig. 4. Proposed structure of the ODA/$PMo_{10}V_2O_{40}^{5-}$ LB film.

3.7. Electrochemical behavior of the $PMo_{10}V_2$ solution and the ODA/$PMo_{10}V_2O_{40}^{5-}$ LB films

3.7.1. Cyclic voltammetry

Reproducible Y-type deposition of ODA/$PMo_{10}V_2O_{40}^{5-}$ LB films onto a glassy carbon electrode is only achieved when the first layer is transferred on the upward traversal of the substrate through the monolayer/air interface. That is, the $PMo_{10}V_2O_{40}^{5-}$ anions are deposited next to the substrate surface. In this way, similar electrochemical behavior is obtained for films with 12 layers and the shape of the CV curves is reproducible. The ODA/$PMo_{10}V_2O_{40}^{5-}$ LB films display a high stability. The stability of the films electrode is examined by measuring the decrease in voltammetric currents during potential cycling of the modified electrode. For example, after potential cycling from +0.4 to −0.8 V at 100 mV s^{-1} in pH 3.18 for 500 scans, a decrease in the cathodic current of 10% is observed. When the ODA/$PMo_{10}V_2O_{40}^{5-}$ LB films are placed in air for several days, almost no change of the electrochemical response of the ODA/$PMo_{10}V_2O_{40}^{5-}$ LB films is observed.

To investigate the influence of ODA cations in LB films on the physico-chemical property of $PMo_{10}V_2O_{40}^{5-}$, the electrochemical behavior of the $PMo_{10}V_2O_{40}^{5-}$ anion in aqueous solution is firstly studied. Fig. 6 shows the cyclic voltammograms of a bare glassy carbon electrode in 1.0×10^{-3} mol l^{-1} of $PMo_{10}V_2O_{40}^{5-}$ acidic solution (curve A) and a glassy carbon electrode deposited with 12 layers of ODA/$PMo_{10}V_2O_{40}^{5-}$ LB films (curve B) in an aqueous solution of pH 3.18. The voltammogram of the $PMo_{10}V_2O_{40}^{5-}$ anion in homogeneous solution shows two reversible waves in the potential range from +0.4 to −0.8 V. The mean peak potentials $E_{1/2}$ ($E_{1/2} = E_{pc} + E_{pa}$) are −0.099 and −0.495 V respectively, and the peak-to-peak separation is less than 0.1 V. Supposing the redox processes are diffusion-controlled behavior of $PMo_{10}V_2O_{40}^{5-}$, then the number of transferred electrons could be obtained from the equation as follows:

$$|E_p - E_{p/2}| = 2.2\frac{RT}{nF} \quad (1)$$

where E_p and $E_{p/2}$ represent the peak potential and the half peak potential, respectively. According to above equation, the n values of the two waves are 0.961 and 1.037, respectively, i.e., the two redox processes are monoelectronic. Compared with curve A, the cyclic voltammogram of the ODA/$PMo_{10}V_2O_{40}^{5-}$ LB film (curve B) presents one reversible redox couple with the mean peak potential $E_{1/2}$ of −0.249 V and the peak-to-

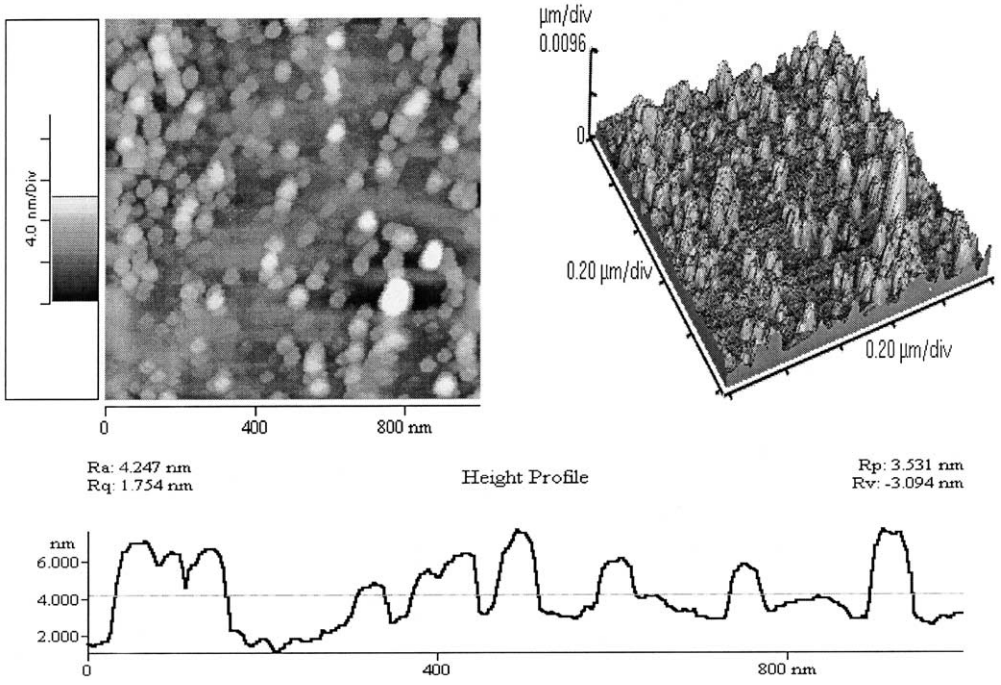

Fig. 5. AFM images of ODA/$PMo_{10}V_2O_{40}^{5-}$ LB film on quartz slide: (A) ichnography; (B) three-dimension; (C) Cross-section.

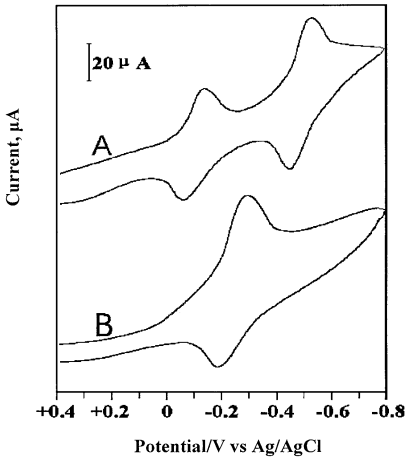

Fig. 6. Cyclic voltammograms of a naked GCE in 1.0 mM $PMo_{10}V_2O_{40}^{5-}$ solution (A) and a GCE deposited with 12 layers of ODA/$PMo_{10}V_2O_{40}^{5-}$ LB film (B) in an aqueous solution of pH 3.18 with a scan rate of 100 mV s^{-1}.

peak separation is more than 0.1 V. To the LB film, it is reasonable to suppose an adsorption-controlled process. According to the equation given below:

$$|E_p - E_{p/2}| = 3.53\frac{RT}{nF} \quad (2)$$

the 1.935 value of n has been calculated. It demonstrates the redox process in the LB film is bielectronic. Because the oxidation capability of Vanadium(V) is stronger than that of Molybdenum(VI), the conclusion could be drawn, that all of the above redox processes can be attributed to the behavior of Vanadium(V).

It is interesting to mention, when the scan rate is not less than 200 mV s^{-1}, the curve of the voltammograms will remain horizontal at a certain range of potential, and the bigger the scan rate, the longer is the horizontal line. However, the CV study of the ODA/$PMo_{10}V_2O_{40}^{5-}$ LB films reveals that several potential sweeps are necessary to make the films fully electroactive, in particular for multilayers. This break in behavior is also observed for pure C_{18}TCNQ [18]. But, even for multilayers, the peak shape of the redox wave is not distorted. These indicate that the redox process is quite fast and unaffected by diffusion of electrolyte ions through a highly hydrophobic film. The relationship between the peak current and the scan rate provides further proof. Fig. 7 represents the relationships between the peak current and the scan rate. From A in Fig. 7, a linear relationship between the first peak current of the voltammograms of the ODA/$PMo_{10}V_2O_{40}^{5-}$ LB film versus the scan rate was observed, which indicates that the redox process exhibits the adsorption-controlled behavior of an electrolyte. This is a surface reaction process. However, B in Fig. 7 displays a linear relationship between the first peak current of the voltammograms of the $PMo_{10}V_2O_{40}^{5-}$ anion in acidic solution versus the square root of scan rate, which demonstrates that this redox process has the diffusion-controlled behavior of the $PMo_{10}V_2O_{40}^{5-}$ anion. The two results testify that the above supposition is true. Since the size of the $PMo_{10}V_2O_{40}^{5-}$ anion is very large, its diffusion rate is small. As the scan rate is not less than 200 mV s^{-1}, the curve of voltammograms will keep horizontal at

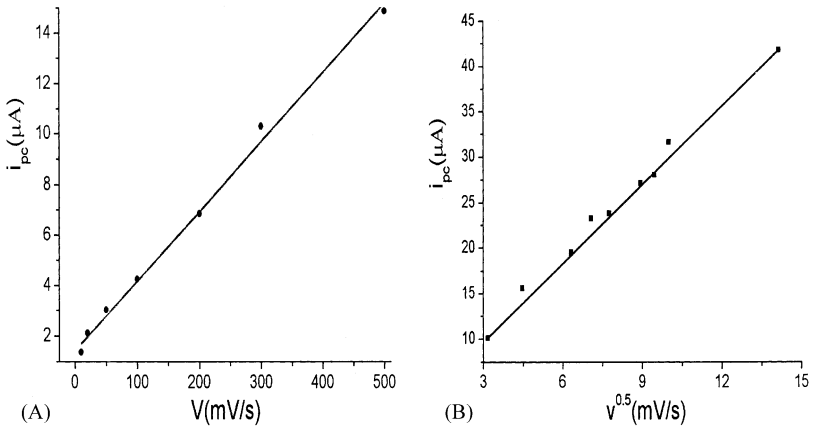

Fig. 7. The relationship between the first peak current of the voltammograms of the ODA/$PMo_{10}V_2O_{40}^{5-}$ LB film versus the scan rate. (B) The relationship between the first peak current of the voltammograms of the $PMo_{10}V_2O_{40}^{5-}$ anion in acidic solution versus the square root of scan rate.

a certain range of potential, and moreover, the bigger the scan rate, the longer is the horizontal line.

Thus it can be seen that the electrochemical reaction of the $PMo_{10}V_2O_{40}^{5-}$anion is quite fast and facile. Multilayer films can be easily reduced and oxidized. So an estimate of the surface coverage of $PMo_{10}V_2O_{40}^{5-}$ anion could be obtained the equation as follows [19]:

$$i_p = n^2F^2\upsilon A\Gamma_0/4RT \quad (3)$$

where Γ_0 represents is the surface coverage of the redox species. According to the above equation, the 12-layer ODA/$PMo_{10}V_2O_{40}^{5-}$ LB film gives a surface coverage of 5.19×10^{-11} mol cm^{-2}, that is 320 $Å^2$ per $PMo_{10}V_2O_{40}^{5-}$ heteropolyanion. Taking into account the radius of the $PMo_{10}V_2O_{40}^{5-}$ heteropolyanion of about 0.5 nm, it suggests that the monolayer surface is not all occupied by the anions deposited on the interface. Thus even in the solid dense packing state enough empty spaces and channels can be presented in the LB film to allow ion transport, which is attributed to the relatively facile redox reaction in the multilayers.

3.7.2. pH dependence

In general, the reduction of heteropoly-anions is accompanied by protonation, and therefore the pH of the solution has a great effect on the electrochemical behavior of heteropolyanions. Fig. 8 shows the cyclic voltammograms of a GCE deposited with 12 layers of ODA/$PMo_{10}V_2O_{40}^{5-}$ LB film at a scan rate of 100 mV s^{-1} in different pH solution. All the cyclic voltammograms have a couple of waves. With an increase of pH, the potential shifts towards the negative direction and the peak current diminishes gradually, which indicates that H^+ does participate in the redox reaction. This phenomenon was also observed for the $PMo_{10}V_2O_{40}^{5-}$ heteropolyanion in aqueous solution with different pH values. The redox process assigned to two-electron reduction of the $PMo_{10}V_2O_{40}^{5-}$ anion is influenced greatly by the pH of solution. The relationship between

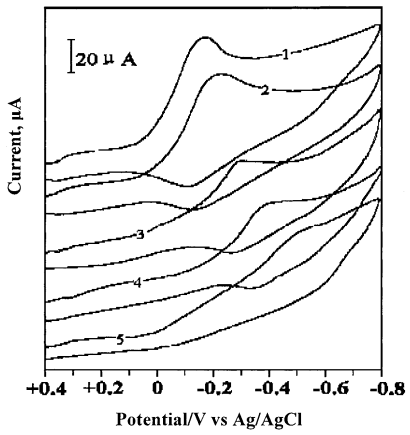

Fig. 8. Cyclic voltammograms of a GCE deposited with 12 layers of ODA/$PMo_{10}V_2O_{40}^{5-}$ LB film at a scan rate of 100 mV s^{-1} in different pH solution (1 → 5): 2.12, 2.95, 4.02, 5.21, 6.42.

the peak potentials and pH values of solution for a GCE deposited with 12 layers of ODA/$PMo_{10}V_2O_{40}^{5-}$ LB film at different pH values was investigated. A linear relationship is observed between the peak potential and the pH values of solution, and the slope of the plot of the peak potential versus pH value (dE_{pc}/dpH) was calculated as −61 mV. This value is close to the theoretical value of −60 mV per pH unit for a $2e^-/2H^+$ process, which confirms further that the two-electron exchange is accompanied by two-protonation reactions in the $PMo_{10}V_2O_{40}^{5-}$ heteropolyanion reduction process. So the electron process can be assigned as follows:

$$PMo_{10}V_2O_{40}^{5-} + 2e^- + 2H^1 \rightleftharpoons H_2PMo_{10}V_2O_{40}^{5-} \quad (4)$$

4. Conclusion

This study has demonstrated that the vanadium-substituted molybdophosphate acid with Keggin struc-

ture, $H_5PMo_{10}V_2O_{40}\cdot 13H_2O$, was synthesized by the method of acidification-etherate. The makeup and structure of this heteropoly acid were charactered by ICP-AES, TG, FT IR, and XRD. The CV behavior of the P–Mo–V heteropoly acid in aqueous solution was studied, which shows that the redox process of the $PMo_{10}V_2O_{40}^{5-}$ anion is quite fast and facile. The voltammogram of the $PMo_{10}V_2O_{40}^{5-}$ anion in homogeneous solution shows two reversible, monoelectronic waves in the potential range from $+0.4$ to -0.8 V. The adsorption properties of vanadium-substituted molybdophosphate on ODA monolayers could be used to form organized molecular assemblies. When the $PMo_{10}V_2O_{40}^{5-}$ anion is added to the subphase, the compression isotherm of ODA is shifted towards a larger cross-section area per molecule and shows a slower rise. AFM images showed that the ODA/$PMo_{10}V_2O_{40}^{5-}$ LB film are relatively homogeneous and without domain structure even after a long time. LAXD data revealed that the ODA/$PMo_{10}V_2O_{40}^{5-}$ LB film possesses a lamellar structure and is well-defined among layers. The calculated results indicate the chain of ODA molecule is almost vertical to the plane of the quartz substrate. UV spectra results showed that the absorption peaks of the ODA/$PMo_{10}V_2O_{40}^{5-}$ LB film are red-shifted compared with the parent solution. This indicates that the $PMo_{10}V_2O_{40}^{5-}$ ions are densely packed and oriented orderly in the film. The CV behavior of the ODA/$PMo_{10}V_2O_{40}^{5-}$ LB film in different pH values shows one reversible, bielectronic waves in the potential range from $+0.4$ to -0.8 V. These quite facile redox reactions demonstrate that there are enough empty spaces and channels existing in the LB films allowing ion transport even in the solid dense packing state. The facile electrochemistry of the LB films could probably be used to prepare a sensitive conducting catalytic electrode and to construct thin film molecular electronic devices based on heteropolyanions in future work.

Acknowledgements

This work was supported by the National Natural Science Foundation of China (No. 29903004). We are also grateful to Ms Wang X.Y. for her help in obtaining the pattern of AFM. Finally, we should like to express thankfulness to Ms Li R. for help and useful discussions.

References

[1] D.K. Lyon, W.K. Miller, T. Novet, P.J. Domaille, E. Evitt, D.C. Johnson, R.G. Finke, J. Am. Chem. Soc. 113 (1991) 7209.
[2] D.E. Katsoulis, M.T. Pope, J. Am. Chem. Soc. 106 (1984) 2737.
[3] N. Mizuno, M. Misono, J. Mol. Catal. 86 (1994) 319.
[4] M. Misono, Catal. Rev. Sci. Eng. 29 (1987) 269.
[5] E.B. Wang, C.W. Hu, L. Xu, Introduction to Polyoxometalate Chemistry, Chemical Industry Press, Beijing, 1998.
[6] W.M. Bu, L. Ye, G.Y. Yang, J.S. Gao, Y.G. Fan, M.C. Shao, J.Q. Xu, Inorg. Chem. Commun. 4 (2001) 1.
[7] J.E. Toth, F.C. Anson, J. Electroanal. Chem. 256 (1988) 361.
[8] S. Dong, M. Liu, J. Electroanal. Chem. 372 (1994) 95.
[9] M. Sadakane, E. Steckhan, Chem. Rev. 98 (1998) 219.
[10] B. Fabre, G. Bidan, M. Lapkowski, J. Chem. Soc., Chem. Commun. 12 (1994) 1509.
[11] L.M. Goldenberg, J. Electroanal. Chem. 379 (1994) 3.
[12] M. Clemente-Leon, B. Agricole, C. Mingotand, C.J. Gomez-Garcia, E. Coronado, P. Delhaes, Langmuir 13 (1997) 2340.
[13] S. Liu, Z. Tang, E. Wang, S. Dong, Thin Solid Films 339 (1999) 277.
[14] G.A. Tsigdinos, C.J. Hallada, Inorg. Chem. 7 (1968) 437.
[15] A. Bielanski, J. Datka, B. Gil, A. Malecka-Lubanska, A. Micek-Ilrricka, Catal. Lett. 57 (1999) 61.
[16] Q.Y. Wu, S.K. Wang, D.N. Li, X.F. Xie, Inorg. Chem. Commun. 5 (2002) 308.
[17] C. Rocchicciolini-Deltcheff, R. Thouvenot, R. Franck, Inorg. Chem. 22 (1983) 207.
[18] M. Beley, J.P. Collin, R. Ruppert, J.P. Sauvage, J. Chem. Soc., Chem. Commun. 19 (1984) 1315.
[19] A.P. Brown, F.C. Anson, Anal. Chem. 49 (1977) 1589.